

Postdetection Switch-and-Stay Combining in Nakagami- m Fading

Sasan Haghani, *Student Member, IEEE*, and Norman C. Beaulieu, *Fellow, IEEE*

Department of Electrical and Computer Engineering, University of Alberta, Edmonton, Alberta, Canada, T6G 2V4

E-mail: haghani@ece.ualberta.ca, beaulieu@ece.ualberta.ca

Abstract—In two recent papers, the performances of dual branch postdetection switch-and-stay combining (SSC) for noncoherent binary orthogonal frequency-shift keying (BFSK) and noncoherent M -ary orthogonal frequency-shift keying (MFSK) operating in the present of slow flat fading modeled by Rayleigh, Nakagami- m , and Rician distributions have been analyzed. This paper shows that the previous analyses of BFSK and MFSK with postdetection SSC in Nakagami- m fading, which was limited to integer values of m , are incorrect and we derive correct bit error rate performance results for BFSK and MFSK with dual-branch SSC in Nakagami- m fading for all values of m . Our analytical results are verified using extensive Monte Carlo simulations. It is shown that for a given bit error rate the performance gain of postdetection SSC over predetection SSC has been overestimated by several dBs in SNR in previous reported work.

I. INTRODUCTION

Two papers [1], [2], recently published, have studied the performance of dual-branch postdetection switch-and-stay combining (SSC) for noncoherent orthogonal binary frequency-shift keying (BFSK) and noncoherent orthogonal M -ary frequency-shift keying (MFSK) in Rayleigh, Nakagami- m and Rician fading channels. These papers are important, in particular, because they quantify the improvement of postdetection SSC over predetection SSC. In this paper, we show that the analyses of [1],[2] for the Nakagami- m model, which are restricted to integer values of m , are mathematically incorrect and we derive correct expressions for the bit error rate (BER) performances of dual-branch SSC with BFSK and MFSK in Nakagami- m fading channels. Furthermore, we show that the results published in [1],[2] overestimate the performance gain of postdetection SSC over predetection SSC by several dBs in SNR for a given BER. Using our analytical results we derive optimum switching thresholds that minimize the error rate performance of BFSK and MFSK with postdetection SSC in Nakagami- m fading.

The remainder of this paper is organized as follows. In Section II, we correct the results published in [1] for the performance of BFSK with postdetection SSC in Nakagami- m fading. Numerical examples are given and it is observed that the performance gain of postdetection SSC over predetection SSC is less than previously reported. In Section III, we correct previous analysis regarding the error rate performance of MFSK with postdetection SSC in Nakagami- m fading published in [2]. Some numerical examples are presented to verify the analyses and the performance of MFSK with postdetection SSC is compared to the performance of MFSK with predetection SSC. In each section, Extensive Monte Carlo simulations are provided to test the validity of our analytical results. Finally, some conclusions are given in Section IV.

II. AVERAGE BER ANALYSIS OF BFSK WITH POSTDETECTION SSC IN A NAKAGAMI- m FADING CHANNEL

The block diagram of a BFSK system with dual-branch postdetection SSC is given in [1, Fig. 1]) and is not repeated here for the sake of brevity. The operation of the switching mechanism and the considerations involved in choosing an optimum switching threshold are discussed in [1, Section III] and a general expression for the average bit error rate (BER) of noncoherent BFSK with postdetection SSC is given in [1, Section IV]. This expression shows that to calculate the probability of error one needs to calculate the CDF of W_1 and W_2 defined as

$$W_1 = W_{11} - W_{12} = E_b^2 |2\alpha_1 e^{j\theta_1} + N_{11}|^2 - E_b^2 |N_{12}|^2 \quad (1)$$

$$W_2 = W_{21} - W_{22} = E_b^2 |2\alpha_2 e^{j\theta_2} + N_{21}|^2 - E_b^2 |N_{22}|^2 \quad (2)$$

where E_b is the energy per bit per symbol, N_{ij} , $i, j = 1, 2$ are independent and identically distributed (i.i.d) zero-mean Gaussian random variables (RVs) with variance $4N_0/E_b$, and $\alpha_i e^{j\theta_i}$, $i = 1, 2$ are the complex channel gains. Note that in obtaining (1) and (2), we have assumed, without loss of generality, that the first symbol in the alphabet is transmitted.

A. Analysis

In [1, p. 1598], the authors have assumed that for Nakagami- m fading and for integer values of m , the RV W_{11} , defined in (1) has a central chi-squared distribution. In the sequel, we show that this is, indeed, incorrect and we find the correct distribution of W_{11} for integer as well as non-integer values of m . Subsequently, we derive the correct BER of BFSK with dual branch postdetection SSC using the general expression given for the average BER of noncoherent BFSK with postdetection SSC given in [1].

Under the Nakagami- m fading assumption, θ_1 in (1) is assumed to be uniformly distributed in $[0, 2\pi)$ and the probability density function (PDF) of α_1 is given by [3, eq. (2.20)]

$$p_{\alpha_1}(\alpha_1) = \frac{2\alpha_1^{2m_1-1}}{\Gamma(m_1)} \left(\frac{m_1}{\Omega_1}\right)^{m_1} \exp\left(-\frac{m_1\alpha_1^2}{\Omega_1}\right) \quad (3)$$

where m_1 is the fading parameter corresponding to channel one, $\Omega_1 = \mathbb{E}(\alpha_1^2)$ and \mathbb{E} denotes the expectation operation. The RV W_{11} can be written as

$$W_{11} = |2\alpha_1 e^{j\theta_1} + N_{11}|^2 = |X + Y_1|^2 + |Y_2|^2 \quad (4)$$

where $X = 2\alpha_1$ and Y_1 and Y_2 are zero-mean Gaussian RVs with variance $\sigma = 2N_0/E_b$. Note that the phase term $e^{j\theta_1}$ is

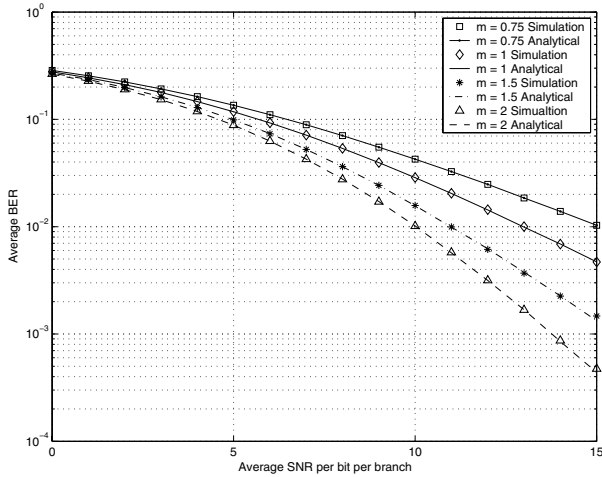


Fig. 1. The average BER of noncoherent BFSK with postdetection SSC versus SNR for $m = .75, 1, 1.5$ and 2 .

absorbed into the noise term N_{11} without changing its statistics [4, p. 292]. Under the static channel condition (fixed α_1), $|X + Y_1|^2$ is a non-central chi-squared RV and $|Y_2|^2$ is a central chi-squared RV. Therefore, W_{11} is a non-central chi-squared RV with two degrees of freedom and its CDF is given by

$$F_{W_{11}}(w) = 1 - Q_1\left(\frac{2\alpha_1}{\sigma}, \frac{\sqrt{w}}{\sigma}\right) \quad (5)$$

where $Q_1(a, b)$ is the first order Marqum Q-function and is defined in [3, eqn. (4.11)]. To completely specify the distribution of $F_{W_{11}}(w)$, we remove the condition that α_1 is fixed by averaging (7) over the pdf of α_1 . After some mathematical manipulations and integral evaluations, this results in

$$F_{W_{11}}(w) = 1 - C_1(m_1, \bar{\gamma}_1) \sum_{k=0}^{\infty} \frac{C_2(k, m_1, \bar{\gamma}_1) \Gamma(k+1, \frac{w}{2\sigma^2})}{k!} \quad (6a)$$

where $\Gamma(a, x)$ is the incomplete Gamma function [5] and

$$C_1(m, \bar{\gamma}) = \frac{\left(\frac{m}{\bar{\gamma}}\right)^m}{\Gamma(m)\left(1 + \frac{m}{\bar{\gamma}}\right)^m} \quad (6b)$$

$$C_2(k, m, \bar{\gamma}) = \frac{\Gamma(m+k)}{k! \left(1 + \frac{m}{\bar{\gamma}}\right)^k}. \quad (6c)$$

The PDF of W_{11} can now be obtained from its CDF as

$$f_{W_{11}}(w) = \frac{C_1(m_1, \bar{\gamma}_1) e^{-\frac{w}{2\sigma^2}}}{2\sigma^2} \sum_{k=0}^{\infty} \frac{C_2(k, m_1, \bar{\gamma}_1) w^k}{k! (2\sigma^2)^k}. \quad (7)$$

Eqn. (7) clearly shows that the PDF of W_{11} is not central chi-squared (compare with [6, eq. (4.39)]).

The RV W_{12} is central chi-square with two degrees of freedom and parameter $2N_0/E_b$. Hence, its PDF is given by

$$f_{W_{12}}(w) = \frac{1}{2\sigma^2} \exp\left(-\frac{w}{2\sigma^2}\right). \quad (8)$$

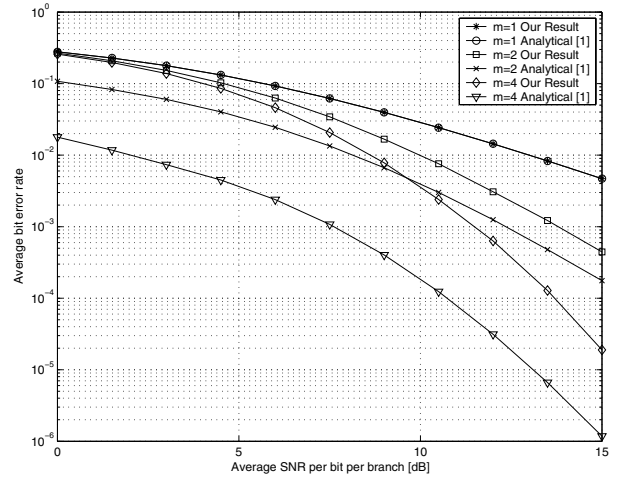


Fig. 2. The average BER of noncoherent BFSK with postdetection SSC versus SNR for $m = 1, 2$ and 4 .

Now, using [6, pp. 185-186], and after much mathematical manipulations, we obtain the CDF of $W_1 = W_{11} - W_{12}$ as

$$F_{W_1}(w) = \begin{cases} 1 - C_1(m_1, \bar{\gamma}_1) e^{-\frac{w}{2\sigma^2}} \\ \times \sum_{k=0}^{\infty} \sum_{n=0}^k \sum_{t=0}^n \frac{C_2(k, m_1, \bar{\gamma}_1)}{2^n t!} \left(\frac{w}{\sigma^2}\right)^t, & w > 0 \\ e^{-\frac{w}{2\sigma^2}} \left[1 - C_1(m_1, \bar{\gamma}_1) \right. \\ \left. \times \sum_{k=0}^{\infty} \frac{C_2(k, m_1, \bar{\gamma}_1) (2^{k+1} - 1)}{2^k} \right], & w < 0 \end{cases} \quad (9)$$

which corrects [1, eq. (41)]. A similar expression can be derived for the CDF of W_2 and the result is equal to (9) where m_1 and $\bar{\gamma}_1$ are replaced with m_2 and $\bar{\gamma}_2$, respectively.

A general expression for the BER of noncoherent BFSK with dual branch postdetection SSC can now be obtained by substituting the CDF of W_1 and W_2 in [1, eq. (8)]. In the case of i.i.d branches $m = m_1 = m_2$, $\bar{\gamma} = \bar{\gamma}_1 = \bar{\gamma}_2$ and the BER reduces to

$$P_b(E) = \left[1 - C_1(m, \bar{\gamma}) \sum_{k=0}^{\infty} \frac{C_2(k, m, \bar{\gamma}) (2^{k+1} - 1)}{2^{k+1}} \right] \\ \times \left[1 - C_1(m, \bar{\gamma}) e^{-\frac{\eta_T \bar{\gamma}}{4}} \sum_{k=0}^{\infty} C_2(k, m, \bar{\gamma}) \right] \\ \times \left\{ \sum_{n=0}^k \sum_{t=0}^n \frac{(\eta_T \bar{\gamma})^t}{2^{n+t+1} t!} - \frac{(2^{k+1} - 1)}{2^{k+1}} \right\} \quad (10)$$

where $\eta_T = \frac{w_T}{E_b^2 \Omega}$ is the normalized switching threshold. Eqn. (10) corrects the BER expression given previously in [2, eqn. (43)] for i.i.d Nakagami- m fading.

For Rayleigh fading, one can show after much mathematical manipulations that (10) reduces to [1, eq. (20)], as expected.

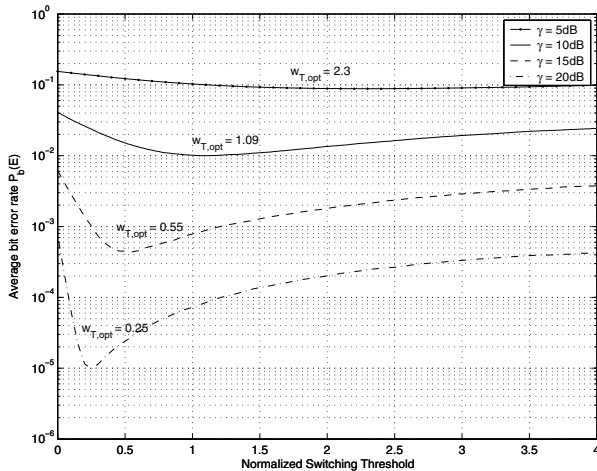


Fig. 3. The average BER of noncoherent BFSK with postdetection SSC versus the normalized switching threshold over i.i.d Nakagami- m fading channels with $m = 2$.

B. Numerical Examples

To further assess the validity of our theoretical results, extensive Monte Carlo simulations have been carried out. For example, Fig. 1 shows the BER performance of postdetection SSC in i.i.d Nakagami- m fading for $m = 0.75, 1, 1.5$ and 2. Fig. 1 clearly shows that there is excellent agreement between the simulation results and the theoretical results obtained from (10).

Fig. 2 shows the BER performance of noncoherent BFSK with postdetection SSC in i.i.d Nakagami- m fading for $m = 1, 2$ and 4 obtained theoretically using (10) and also from simulation together with the analytical results given in [1] also for $m = 1, 2$ and 4. We point out that no simulation results were presented in [1]. Fig. 2 clearly shows that the results of [1] are only correct for $m = 1$ which corresponds to Rayleigh fading. For other values of m the results of [1] overestimate the performance of the system by several dBs in SNR. For example, for $m = 2$ and at a BER of 10^{-2} the SNR difference between the correct result and the incorrect result is 1.842 dB. For $m = 4$ and at a BER of 10^{-4} , the SNR difference between the correct result and the incorrect result is 3.318 dB. Note, importantly that to obtain the results of Figs. 1 and 2, the optimal switching threshold is calculated for each value of SNR numerically. Fig 3 shows the average BER of noncoherent BFSK with postdetection SSC versus the normalized switching threshold for i.i.d Nakagami- m fading with $m = 2$ for several values of average SNR. This figure shows that an optimum threshold exists for every SNR value and that the optimum threshold decreases as the average SNR increases. This optimal value can be obtained by solving

$$\left. \frac{dP_b(E)}{d\eta_T} \right|_{\eta_T=\eta_T^*} = 0. \quad (11)$$

Substituting (10) in (11), and after some mathematical manipulation, one obtains

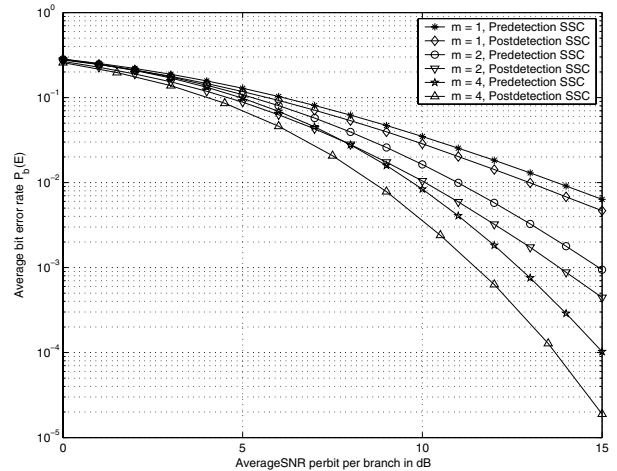


Fig. 4. Comparison of the average BER of noncoherent BFSK in i.i.d Nakagami- m fading with predetection and postdetection SSC for $m = 1$ and $m = 2$.

$$\begin{aligned} & -\frac{\bar{\gamma}}{4} \exp\left(-\frac{\bar{\gamma}\eta_T}{4}\right) \sum_{k=0}^{\infty} \frac{C_2(k, m, \bar{\gamma})(2^{k+1} - 1)}{2^{k+1}} \\ & -\frac{\bar{\gamma}}{4} \exp\left(\frac{\bar{\gamma}\eta_T}{4}\right) \sum_{k=0}^{\infty} \sum_{n=0}^k \frac{\Gamma(n+1, \bar{\gamma}\eta_T/2)}{n!2^{n+1}} \\ & +\frac{\bar{\gamma}}{2} \exp\left(-\frac{\bar{\gamma}\eta_T}{4}\right) \sum_{k=0}^{\infty} \sum_{n=0}^k \frac{(\bar{\gamma}\eta_T)^n}{n!2^{2n+1}} = 0. \end{aligned} \quad (12)$$

The root of (12) is the optimum switching threshold. Eqn. (12) corrects [1, eq. (45)].

Fig. 4 compares the optimal average BERs of noncoherent BFSK with predetection and postdetection SSC for Nakagami- m channels with $m = 1, 2$ and 4. Fig. 4 shows that as the SNR increases, the gain of postdetection SSC increases over the gain of predetection SSC. Furthermore, for a given BER, the SNR difference in performance between predetection SSC and postdetection SSC increases as the fading parameter, m , increases. For example, at a BER of 10^{-2} and for $m = 2$, the SNR difference between predetection and postdetection SSC is 0.8 dB while at the same SNR and for $m = 4$ the SNR difference between predetection SSC and postdetection SSC is 1.1 dB. This is expected, since increasing the m parameter results in a better channel, as does also increasing the SNR.

Fig. 4 also shows that at a given BER the SNR difference between predetection and postdetection SSC is less than the SNR difference reported in [1, Fig. 10]. For example, at a BER of 10^{-3} and $m = 2$, the SNR difference between predetection and postdetection SSC, as shown in Fig. 4, is only 1.1 dB, whereas in [1, Fig. 10], the SNR difference is 2.0 dB.

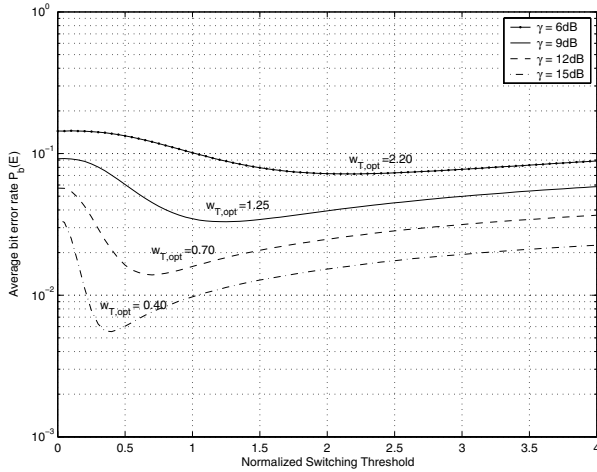


Fig. 5. The average SER of noncoherent QFSK over i.i.d Nakagami- m fading channels with postdetection SSC versus the normalized switching threshold with $m = 0.75$.

III. AVERAGE SER ANALYSIS OF MFSK WITH POSTDETECTION SSC IN A NAKAGAMI-M FADING CHANNEL

A. Analysis

A block diagram of a MFSK system with dual-branch post SSC is shown in [2, Fig. 1] and is not repeated here for the sake of brevity. The switching mechanism is the same as that explained in [1]. A general expression for the average symbol error rate (SER) of noncoherent MFSK with dual-branch SSC is given in [2, eq. (8)]. This expression shows that to calculate the SER one needs to know the PDFs and CDFs of W_{ij} , $i = 1, 2, j = 1, \dots, M$ as shown in [2, Fig. 1] and defined as [2]

$$W_{11} = E_s^2 |2\alpha_1 e^{j\theta_1} + N_{11}|^2 \quad (13)$$

$$W_{21} = E_s^2 |2\alpha_2 e^{j\theta_2} + N_{21}|^2 \quad (14)$$

$$W_{jm} = E_s^2 |N_{jm}|^2, \quad j = 1, 2, m = 2, \dots, M \quad (15)$$

where E_s is the energy per symbol, θ_i , $i = 1, 2$ are uniformly distributed in $[0, 2\pi)$, α_i , $i = 1, 2$ are Nakagami- m distributed and N_{ij} , $i = 1, 2, j = 1, \dots, M$ are i.i.d zero-mean, complex Gaussian RVs with variance $4N_0/E_s$.

In [2], the authors have mistakenly assumed that the RVs W_{11} and W_{21} are central chi-squared. Using similar analyses to that in the previous section, we derive the correct PDFs and CDFs of W_{11} and W_{21} as

$$f_{W_{1i}} = \frac{C_1(m, \bar{\gamma}_i) e^{-\frac{w}{2\sigma^2}}}{2\sigma^2} \sum_{k=0}^{\infty} \frac{C_2(k, m, \bar{\gamma}_i) w^k}{k!(2\sigma^2)^k}, \quad i = 1, 2 \quad (16)$$

and

$$F_{W_{1i}}(w) = 1 - C_1(m, \bar{\gamma}_i) \times \sum_{k=0}^{\infty} \frac{C_2(k, m, \bar{\gamma}_i) \Gamma(k+1, \frac{w}{2\sigma^2})}{k!}, \quad i = 1, 2 \quad (17)$$

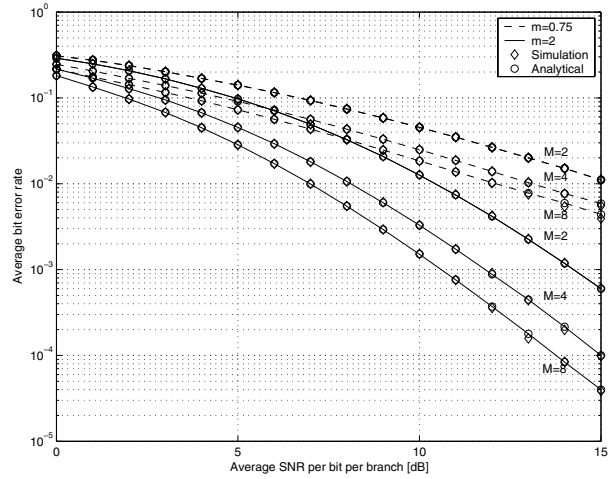


Fig. 6. The average BER of noncoherent MFSK as a function of average SNR per bit per branch in i.i.d Nakagami- m fading with postdetection SSC for $M = 2, 4$ and 8 and for $m = 0.75$ and 2 .

respectively, where $\sigma^2 = 2E_b N_0$. The PDFs and CDFs of W_{jm} , $j = 1, 2, m = 2, \dots, M$ can be shown to be

$$f_{W_{jm}}(w) = \frac{1}{2\sigma^2} \exp\left(-\frac{w}{2\sigma^2}\right), \quad j = 1, 2, \quad m = 2, \dots, M \quad (18)$$

$$F_{W_{jm}}(w) = 1 - \exp\left(-\frac{w}{2\sigma^2}\right), \quad j = 1, 2, \quad m = 2, \dots, M. \quad (19)$$

Substituting (16)-(19) in the general SER expression given in [2] one obtains the correct SER in the case of Nakagami- m fading. For the i.i.d case, after some mathematical manipulation and integral evaluations, the SER simplifies to

$$P_s(E) = 1 - C_1(m, \bar{\gamma}) \sum_{k=0}^{\infty} \sum_{l=0}^{M-1} (-1)^l \binom{M-1}{l} \frac{C_2(k, m, \bar{\gamma})}{k!(l+1)^{k+1}} \times \Gamma\left(k+1, \frac{(1+l)\bar{\gamma}\eta_T}{4}\right) - \left\{ 1 - C_1(m, \bar{\gamma}) e^{-\frac{\bar{\gamma}\eta_T}{4}} \right. \\ \times \sum_{k=0}^{\infty} C_2(k, m, \bar{\gamma}) \sum_{n=0}^k \frac{(\bar{\gamma}\eta_T)^n}{4^n n!} \left. \right\} \left(1 - e^{-\frac{\bar{\gamma}\eta_T}{4}} \right)^{M-1} \\ \times C_1(m, \bar{\gamma}) \sum_{k=0}^{\infty} \sum_{l=0}^{M-1} (-1)^l \binom{M-1}{l} \frac{C_2(k, m, \bar{\gamma})}{(l+1)^{k+1}} \quad (20)$$

where, $\eta_T = \frac{w_T}{\Omega E_s^2}$ is the normalized switching threshold. Note that (20) corrects [2, eq. (36)] for i.i.d Nakagami- m fading. Note that for orthogonal MFSK, the BER can be related to the SER by $P_b(E) = \frac{M}{2(M-1)} P_s(E)$ [4].

For $m = 1$, which corresponds to i.i.d Rayleigh fading, it can be shown after much mathematical manipulations that (20) reduces to [2, eq. (16)], as expected.

B. Numerical Examples

Fig. 6 shows the BER performance of MFSK with postdetection SSC for $M = 2, 4$ and 8 over i.i.d Nakagami- m fading

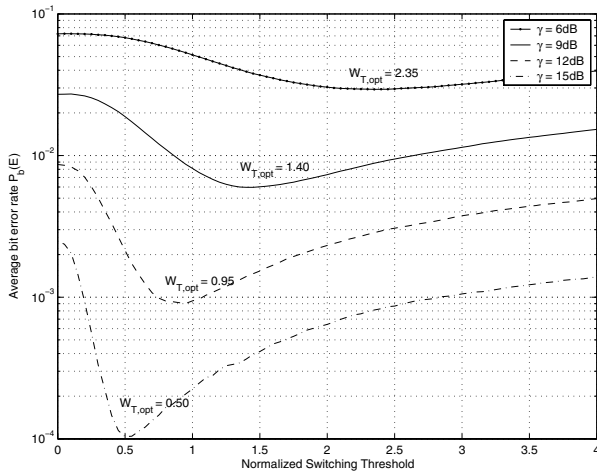


Fig. 7. The average SER of noncoherent QFSK over i.i.d Nakagami- m fading channels with postdetection SSC versus the normalized switching threshold with $m = 2$.

with $m = 0.75$ and $m = 2$ as a function of SNR per branch per bit obtained from simulation and the theoretical results given in (20). Fig. 6 confirms the validity of our results. Note that the results of Fig. 6 are obtained by calculating the optimal threshold value for each value of SNR.

A figure similar to Fig. 2, comparing the results obtained in (20) and [2, eq. (36)] could not be produced simply because the theoretical expression given in [2, eq. (36)] gives values that are outside plots having any reasonable axes scales.

Figs. 5 and 7 show the average SER of noncoherent 4-ary FSK over i.i.d Nakagami- m fading channels with postdetection SSC as a function of the normalized switching threshold for $m = 0.75$ and $m = 2$ and for several values of SNR, respectively. For each value of SNR, the optimum switching threshold is reported on the figures. Figs. 5 and 7 show that an optimum threshold exists for each value of SNR. Similar to [2, Fig. 1], which is obtained for i.i.d Rayleigh fading, the optimal switching threshold is a decreasing function of the average SNR. This implies that when the SNR is larger the system will switch more often to exploit better fading conditions on the other channel [2]. Figs. 5 and 7 also show that for each value of SNR, as the fading parameter, m , increases the optimal threshold value increases. For example, at an average SNR of 15 dB and for $m=0.75$ and 2, the optimal switching threshold is 0.38 and 0.55, respectively. Thus, the system will switch less frequently when operating in lightly faded channels than when operating in severely faded channels.

It is important to compare the performance of postdetection and predetection SSC combining in fading channels. For predetection SSC, an analytical expression for the SER performance of MFSK with predetection SSC is given in [2, eq. (37)]. Using [2, eq. (37)] and (20), the average BER of noncoherent MFSK with predetection and postdetection SSC is plotted in Fig. 8 for $M = 2, 4$ and 8 as a function of the average SNR per bit per branch with fading parameter $m = 0.75$ and $m = 2$. In Fig. 8, the optimum switching threshold is obtained for each value of

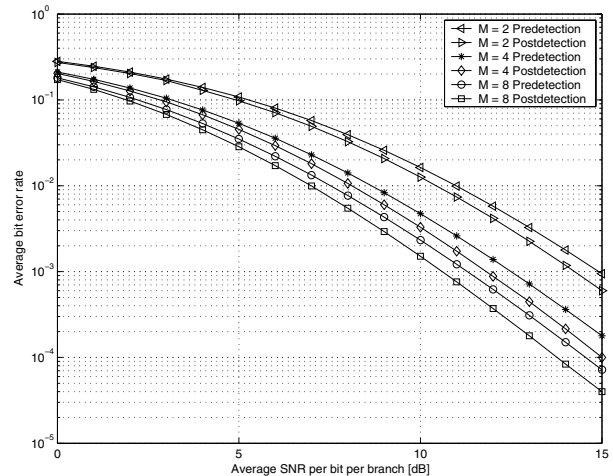


Fig. 8. The average BER of noncoherent MFSK as a function of average SNR per bit per branch with predetection and postdetection SSC for $M=2, 4$ and 8. The branch fading are i.i.d Nakagami with $m = 2$.

SNR for both predetection SSC and postdetection SSC combining. As expected, postdetection SSC outperforms predetection SSC for all values of SNR. Also, Fig. 8 shows that the performance difference between predetection and postdetection SSC increases slightly as M increases. For example, at a BER of 10^{-3} the SNR difference between predetection SSC and postdetection SSC is 0.6 and 0.7 dB for $M = 2$ and $M = 8$, respectively.

IV. CONCLUSION

In this paper, we have corrected previous results published on the performances of BFSK and MFSK with dual-branch postdetection SSC combining in Nakagami- m fading channels. Optimum switching thresholds for minimizing the BER of BFSK and MFSK with postdetection SSC have been derived. We have also compared the performances of BFSK and MFSK with predetection and postdetection SSC in Nakagami- m fading channels. It was observed that postdetection SSC outperforms predetection SSC for all values of SNR, though the performance differences are less than previously reported.

REFERENCES

- [1] M.-S. Alouini and M. K. Simon, "Postdetection Switched Combining- A Simple Diversity Scheme With Improved BER Performance," *IEEE Trans. Commun.*, vol. 51, pp. 1591–1602, Sept. 2003.
- [2] M. K. Simon and M.-S. Alouini, "Probability of Error for noncoherent M -ary orthogonal FSK With Post-detection Switched Combining," *IEEE Trans. Commun.*, vol. 51, pp. 1456–1462, Sept. 2003.
- [3] M. K. Simon and M.-S. Alouini, *Digital Communication over Fading Channels: A Unified Approach to Performance Analysis*. New York: Wiley, 2000.
- [4] J. G. Proakis, *Digital Communications*, 2nd ed. New York: McGraw-Hill, 1989.
- [5] I. S. Gradshteyn and I. M. Ryzhik, *Table of Integrals, Series and Products*, 6th ed. San Diego, CA: Academic Press, 2000.
- [6] A. Papoulis and S. U. Pillai, *Probability, Random Variables and Stochastic Processes*, 4th ed. New York, USA: McGraw-Hill, 2002.